

Identifying Climatic Change Adaptations of Crops in Orinoco Basin Oxisols Through Study of Soil Water Availability

Oscar Javier Gallo^{1*}, Juan Carlos Loaiza-Usuga², Betty Jazmín Gutiérrez Rodríguez³, Andrés Javier Peña Quiñones¹, Jaime Humberto Bernal Riobo¹

¹ Network of Annual and Agro-Industrial Crops, Corporación Colombiana de Investigación Agropecuaria (AGROSAVIA), La Libertad, Villavicencio, Meta, Colombia

² Departamento de Geociencias y Medioambiente, Sede Medellín, Facultad de Minas, Universidad Nacional de Colombia, Carrera 80 No 65-223, Bloque M2. Office 312, Campus Robledo, 050036, Medellín, Colombia

³ Intelligence Analyst and Scientific and Technological Dissemination, Corporación Colombiana de Investigación Agropecuaria (AGROSAVIA), Bogotá DC, Colombia

* Corresponding author's e-mail: ogallo@agrosavia.com

ABSTRACT

Crop yield variations in the Orinoquía region – Colombia, are primarily associated with extreme precipitation events. Therefore, studying crop water supplies under naturally variable climate conditions is fundamental in an actual climatic change context. Rainfall data collected in the Quenane sub-basin were analyzed to understand the soil water dynamics in the Orinoco catchment. The basin covers 179 km² and consists of the piedmont landscape (Eastern Mountain Range) of the Villavicencio Municipality, Department of Meta. This study analyzes the rainfall variability using Pearson correlation analysis, the Mann-Kendall trend analysis, and soil water balance to determine the implications of these factors in crop performance at the basin scale. The results indicated that the spatial distribution of rainfall in the basin responds to a longitudinal average variation of precipitation and that this response is more accentuated (i.e., greater rainfall) toward the west of the basin. Despite the basin being located in the tropical zone, no evidence was found regarding the effect of the El Niño Southern Oscillation on rainfall patterns. Yet, the temporal analysis revealed some years with extreme rainfall values and high-uncertainty levels during transitions between wet and dry periods. During these transition periods, a greater potential for effects on farm yields exists due to the variable cumulative rainfall observed during recent years. The time series trend analysis revealed changes in rainfall patterns at different scales (weekly and yearly) and distribution based on the decrease of rainy days per week and year. This trend is much more accentuated during the second half of the year, generating uncertainty and reducing farm yields throughout the basin.

Keywords: soil moisture, savanna, water balance, climatic change, tropic environments.

INTRODUCTION

The Intergovernmental Panel on Climate Change (IPCC) proposed scenarios in which global droughts are expected to directly affect the global quality and availability of water resulting in considerable challenges and impacts on society, environments, ecosystems, and plants growth and development (Hoogenboom, 2000; Qiu et al., 2023). Therefore, understanding the relationship between weather variables, and crop yields and production, is crucial to prepare for climate

variations. Presently, the challenge of the climate change threat is to identify the coming threats to agroecosystems and food systems (IPCC, 2020). Following threat identification, it will be possible to determine the best adaptation strategies, a topic that several authors identify as critical in the next few years (Cui, 2020; Pathak, 2023; Qiu et al., 2023). In current high-uncertainty scenarios, adaptation to climatic variations is more necessary than strategy development (Cui, 2020; Egerer et al., 2021; Ibrahim and Johansson, 2021). The need for adaptation should be considered a

milestone in the pathway toward increased food production (food security) and reduced environmental impact. This begins with the reduction of greenhouse gas emissions through the implementation of the climate-smart agriculture (CSA) approach (Mahlengule Zwane, 2019; Ross, 2016).

In the Colombian context, Orinoquía region is renowned as the last agricultural frontier (UPRA, 2018), and their products supply most of the cities in the country. Furthermore, this region has the challenge of producing cereals, fibers, bioenergy, meat, and milk within the CSA context (Ramirez-Contreras et al., 2022). The primary climate feature of the Orinoco basin is the abundant rainfall, characterized by a monomodal rainfall regime with more than 2000 mm per year (Bustamante, 2019). This allows two annual crop cycles and considerable forage production (Fontanilla-Díaz et al., 2021). However, despite the large volume of precipitation per area unit, it is insufficient to guarantee annual crop water requirements, and water scarcity, associated with soil characteristics and rainfall distribution, has been reported by Galvis Quintero et al. (2018).

Varying regional rainfall patterns, related to fluctuations in annual accumulated precipitation determine crop production success or failure (Das et al., 2024). The effect of rainfall pattern variability on crop productivity is associated with the prevalence of rainfed agricultural systems. For example, rice produced under rainfed conditions is highly susceptible to soil water deficits, especially during certain phenological stages, and is therefore severely affected by water scarcity (Pardo et al., 2020; Zhu et al., 2023). In addition to the direct effect of precipitation on plants, there is also an indirect effect on the dynamic population of pests and diseases, such as bacterial panicle blight (BPB) in rice, a disorder caused by *Burkholderia glumae* and *Burkholderia gladioli* (Hoyos et al., 2013). The presence of BPB in the region has reportedly been associated with the increase in air temperature and humidity, as well as high rainfall, a climatic phenomenon associated with the negative phase of El Niño Southern Oscillation (ENSO) – La Niña. Another indirect effect of climate change on crops is the damage to the native savanna and grasslands associated with increases in the *Rhammatocerus schistocercoides* (langosta llanera) population during dry years (Leon et al., 2018).

Fires are common in savannas during the dry season and propagate easily in grasslands. They

consume forest patch borders, affecting their stability, shape, and spatial distribution at ecological and geomorphological scales (Hébert-Dufresne et al., 2018). Under climate change scenarios, the number of fires could increase, associated with rainfall pattern changes and prolonged dry seasons. This favors the frequency and severity of fires, and by extension, transforms forest areas into savannas (Armenteras et al., 2021; de Oliveira-Júnior et al., 2021).

Worldwide, understanding of climate change and its relationship with agriculture has increased. However, the information generated in tropical zones is poorly understood, and new information is useful for decision-making in agri-food systems. This work analyzes the effects of temporal variation in rainfall on the soil water content and its availability for semiannual crops and grassland in the Caño Quenane sub-basin of the Orinoco catchment. The results of these analyses will support crop planning based on water needs in these tropical savannas.

MATERIALS AND METHODS

Site description

This study was conducted in the Quenane River sub-basin, which has a total area of 185 km². It is located in the foothills of the Colombian Orinoquía region (Colombian Eastern Plains) in the department of Meta in the municipality of Villavicencio (Figure 1). The length of the sub-basin is 54 km and the altitude ranges from 199 to 375 m.a.s.l. The slope oscillates between 0% and 3%, which is typical of plain areas in eastern Colombian (Lozano, 2014). According to Soil Survey Staff (2022), the soils are Typic Hapludox (75%), with inclusions of Oxic Dystropepts (15%) and Typic Kandiudults (10%). The soil usages consist of extensive cattle ranching in natural and introduced pastures, along with several areas of cereals, citrus, oil palm, mandioca, and banana plantations.

The average annual rainfall of the Quenane River sub-basin is 2917 mm, distributed throughout the year following a monomodal pattern with the dry season between December and March and the rainy season from March to November. The mean annual air temperature is 25.8 °C, while the mean minimum and maximum air temperatures are 21.7 °C to 30.8 °C, respectively. The

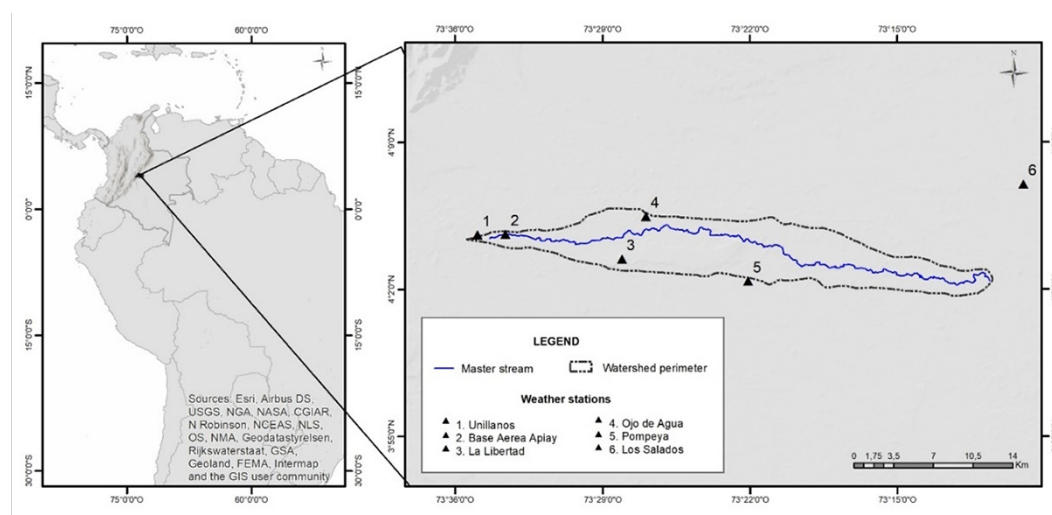


Figure 1. Location of the study area

relative humidity of the air oscillates between 68% to 85% in the dry and rainy seasons, respectively; with mean wind speed lower than 2 m/s (Bernal et al., 2013). The climate in the basin is classified as tropical rain forest (monsoon) in the Köppen system, warm humid climate in the Caldas-Lang classification system, and super humid according to Thornthwaite.

Sampling

Daily rainfall data (mm) were registered in the weather stations located in the basin (Table 1). The information is available in the DHIME database (<http://dhime.ideam.gov.co/atencionciudadano/>), administered by the Colombian Weather Service (IDEAM). Data quality control was conducted (Mesri et al., 2013) and the calculation of daily time series was based on Markov chains (Chica et al., 2014). In addition to precipitation, data on other weather phenomena, such as air temperature (°C), relative air humidity (%), wind speed (m/s), and sunshine (h/day), were provided by La Libertad AGROSAVIA weather

station. These data were used for the analysis. The daily reference evapotranspiration (ET_0) was calculated using the Penman-Monteith method (Allen et al., 1998), based on data from other weather variables using FAO’s ETo Calculator, version 3.1 (The Food and Agriculture Organization, Rome, Italy).

Precipitation analysis

The spatial rainfall variability in the basin was characterized using data from the period 1995 to 2021. After analyzing six stations, the three stations of Unillanos, La Libertad, and Pompeya were selected for use in the analyses. Several statistical tests were conducted using the average annual precipitation data to evaluate normality, homogeneity, and repeated data. The Shapiro-Wilk test was used to evaluate normality, homogeneity with Levene’s test (p value = 0.51) and means comparison using a t -test. The Wilcoxon test was used for repeated data with the two-tailed test, and the Bonferroni correction for contrasts using the open-source Pingouin 0.5.3

Table 1. Weather stations in the Caño Quenane basin

Station	Code*	Type*	Data period
Unillanos	35035070	Main Climatic	1983-2020
Base Aerea Apiay*	35035010	Secondary Synoptic	1968-2016
La Libertad	35025020	Main Climatic	1972-2023
Ojo De Agua	35030050	Rain Gauge	1978-2019
Pompeya	35020060	Rain Gauge	1978-2020
Los Salados*	35020070	Rain Gauge	1968-1994

Note: suspended, +according to IDEAM classification.

for Python 3 package (Vallat 2018). Temporal precipitation variability within the basin was described using the La Libertad station data series. The monthly analysis (temporarily established for the ENSO) of the variation of the interannual patterns of rainfall and anomalies was conducted through a comparison of annual anomalies with the Oceanic Niño index (ONI), the multivariate ENSO index (MEI), the southern oscillation index (SOI), and the sea surface temperature in the Eastern Pacific (SST1 + 2), all according to Peña et al. (2011). A simple linear regression was applied to the monthly values of the indices and the accumulated precipitation, rainy days, mean sunshine, mean temperature, mean maximum temperature, and mean minimum temperature data (Ramirez et al., 2018). A causality test was performed to determine which data series provided the best prediction. In this case, the probability criterion was used to identify significance (Attanasio et al., 2013). The rainfall characterization was performed using a weekly scale (Alan et al., 2014). The distribution of rainfall was analyzed using heat map graphs (Praveen et al., 2020) to describe the weekly accumulated precipitation from 1972 to 2020. The precipitation and evapotranspiration reference values for dry, average, and wet years were plotted and the historical precipitation record data from 25, 50, and 75% quantiles were selected (López et al., 2019).

Rainfall trend analysis

The weekly and annual trend analysis was performed for the precipitation series (La Libertad station) considering accumulated rainfall dependence on stationarity (mean and variability remaining constant) or autocorrelation of the rainfall series. Correlograms containing bands with 95% confidence intervals were generated using the methodology of Gao et al., (2020); thus, defining if there were any levels of autocorrelation associated with certain lags. To determine whether the series did not exhibit autocorrelation or stationarity, the non-parametric Mann–Kendall test was conducted (Bera et al., 2021). This test has been widely used in equatorial conditions by (Bernal et al., 2013; Peña et al., 2011). When autocorrelation was identified in the series, the modified Mann–Kendall test with the pre-whitening method was conducted (Yue and Wang, 2002). Two significance levels were used to define the trend: highly significant (5% significance level)

and significant (10% significance level)(Gao et al., 2020). To analyze the magnitude of the trend, the Sen slope (Z) was estimated; with positive and negative “ Z ” values being associated with increasing and decreasing trends, respectively (Chisanga et al., 2023)

Water supply at ground level

The agricultural water balance was used to determine the soil moisture content available for cultivation at daily scales. A simplification of the balance is shown in Equation 1 (Allen et al., 1998).

$$SMC_i = SMC_{i-1} + EP_i - ETa_i \quad (1)$$

where: SMC_i is the soil moisture content on the current day, SMC_{i-1} is the soil moisture content on the previous day, EP_i is the current effective precipitation, and ETa_i is the current actual evapotranspiration.

The EP is the fraction of rain that reaches the root zone and is calculated based on net rainfall (de Boer-Euser et al., 2016) and the average capacity of the water to reach deep layers in the soil as reported by USDA-SCS (Dastane, 1978). It is noteworthy that CHi (soil water storage) acquires values that range between 0% and the maximum water storage capacity (MWSC) in the soil. For calculating MWSC, local field capacity (FC), permanent wilting point (PWP), and soil depth values were used (Soil Survey Staff, 2022)

The crops used in this study were rice (*Oryza sativa* L.), corn (*Zea mays* L.), soy (*Glycine max* L.), and pasture grass (*Brachiaria decumbens* syn. *Urochloa decumbens*). The establishment of the semiannual crops occurred on April 15 and August 15. The grassland is a permanent cover with a 30-day rotational grazing system. The ET_0 and crop coefficients (K_c) were used to calculate actual evapotranspiration (ETa) (Allen et al., 1998; da Silva et al., 2019). The crop coefficient values (K_c) for each developmental stage are shown in Table 2.

Based on the soil water balance, each day of the crop cycle was classified as either: (a) days with sufficient moisture levels for crop development ($0 \leq CHi \leq MWSC$), (b) days with excess moisture ($CHi \geq MWSC$), and (c) days with deficient moisture ($MWSC = 0$). The amount of water (mm) in excess or deficient was determined according to soil water availability.

Table 2. Crop coefficient (Kc) and days of duration of life cycle stages

Crop	Kc initial	Kc development	Kc mean	Kc end
Rice (120) *	0.40 (20)	1.05 (60)	1.20 (25)	0.60 (15)
Corn (130) *	0.40 (15)	0.80 (41)	1.20 (54)	0.40 (20)
Soybean (110) *	0.35 (20)	0.75 (22)	1.15 (43)	0.60 (25)
Pasture (30) *	NA	0.40 (15)	1.05 (15)	NA

Note: (*) days of duration of life cycle, () days of duration of stages.

RESULTS

Precipitation variability

The average annual precipitation measured at the six weather stations in the Quenane sub-basin was 2752 mm. However, there were zones where the rainfall was higher than 3477 mm/year (7% basin) and others where it was lower than 2472 mm/year (11% basin). The basin’s precipitation gradient lies in an east-west direction, with humid zones toward the mountain range (west) represented by Unillanos station (highest rainfall). The Los Salados station recorded the lowest rainfall values and represented the pattern in the less humid plains (east), Figure 2.

The annual rainfall difference between stations was approximately 1000 mm year⁻¹, and the greatest spatial distance was 54 km between stations. There were significant differences in mean annual precipitation among the stations located in the middle zone (La Libertad and Pompeya), and those in the basin extremes which were 11

km away (Table 3). The regression coefficients associated with ENSO indices (ONI, MEI, SOI, and TSM1 + 2) and climate elements at monthly scales were not significant, Table 4. Unlike in most of Colombia, the temporal variations in monthly rainfall values were unrelated to ENSO (Ramirez et al., 2018). Yet, positive, and negative rainfall anomalies are possible during “El Niño” or “La Niña” events. For example, during negative ENSO phases in 1998 and 2015, rainfall exhibited positive anomalies (excess), and during positive ENSO phases in 2010 and 2013, rainfall exhibited negative anomalies (dry), the primary pattern reported for Colombia. However, between 2016 and 2020, rainfall anomalies (both positive and negative) in the catchment did not match with the ENSO phase occurrences (Figure 3).

Rainfall implications in temporary crops and grasslands

The rainy season lasts approximately 36 weeks, and from week 13 to week 48 (Figure

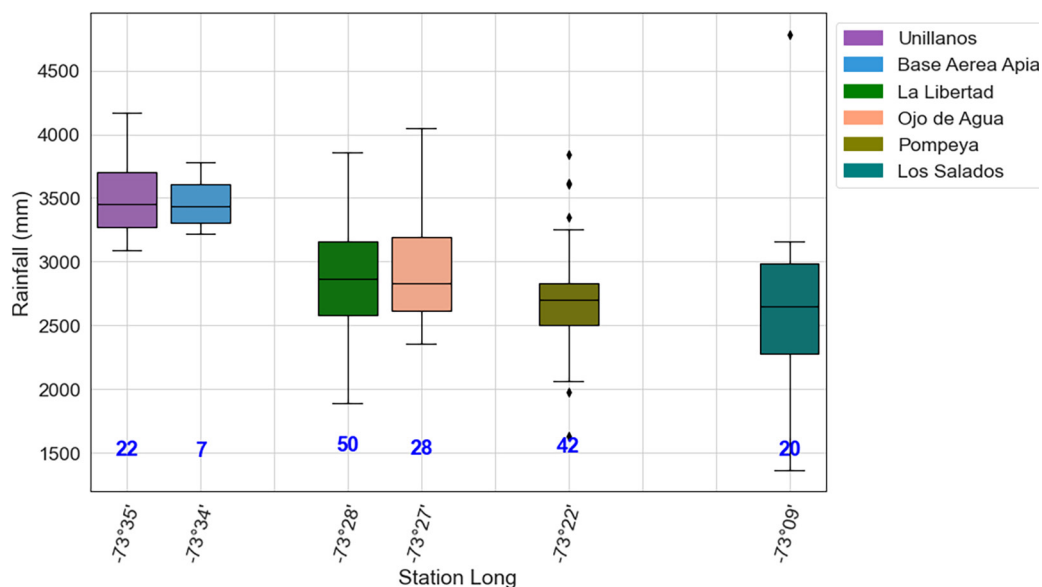


Figure 2. Box plot of annual precipitation in the Caño Quenane sub-basin (numbers in blue: number of years analyzed)

Table 3. Difference in precipitation between selected stations

Contrast	A	B	T	p-unc	p-corr	BF10	Effect size
Station	La Libertad	Pompeya	2.593	0.015	0.015	3.246	0.452
Station	La Libertad	Unillanos	-13.033	0	0	1.16E+10	-1.789
Station	Pompeya	Unillanos	-9.934	0	0	42610000	-2.112

Table 4. Correlation of climatic elements with ENSO indices on a monthly scale

Weather elements	ONI	MEI	SOI	TSM+2
Precipitation (mm)	0.04	0.03	-0.04	0.06
N° days precipitation	-0.01	0.00	0.00	0.02
Maximum temperature	0.10	0.09	-0.06	0.08
Medium temperature	0.12	0.11	-0.08	0.11
Sunshine	0.02	0.01	-0.01	-0.01

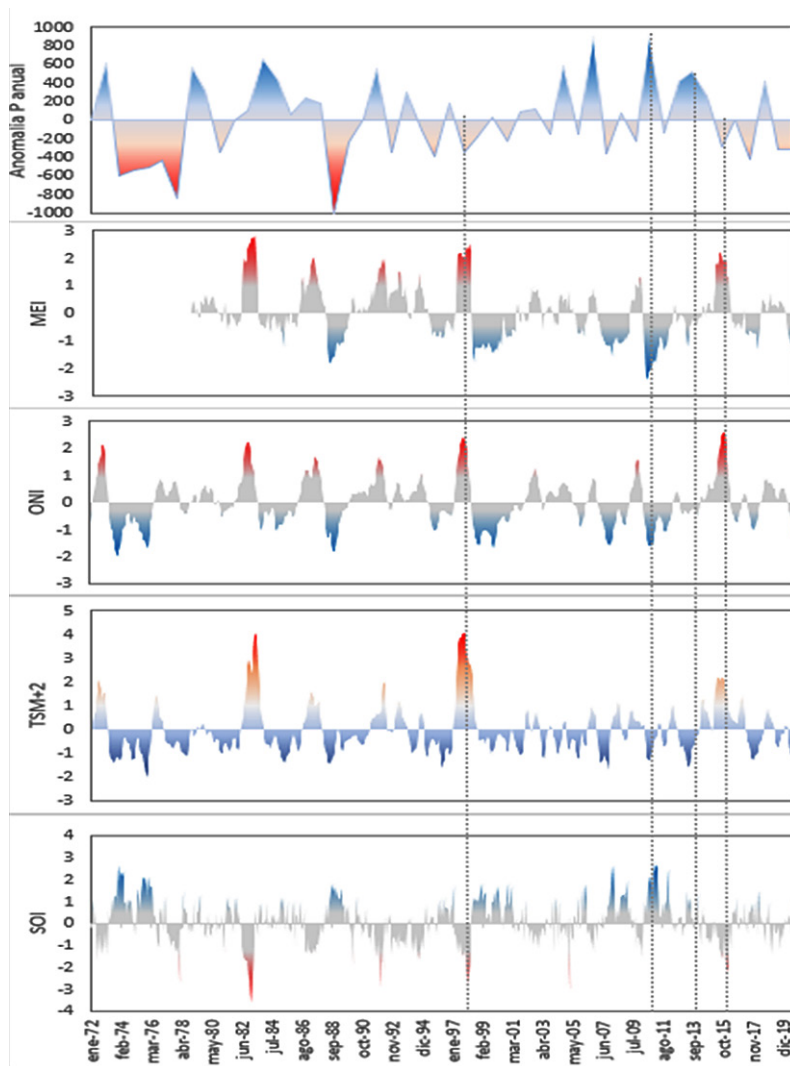


Figure 3. Annual precipitation anomalies and ENSO indices in the Caño Quenane sub-basin

4), rainfall behavior is related to the Intertropical Confluence Zone (ITCZ) (Poveda et al., 2020; Waliser and Jiang, 2015). The rainy season has two short rainy periods related to ITCZ phenomena. The first rainy period occurs between weeks

13 to 33, with rainfall reaching maximum values between weeks 17 to 26. The second rainy period (between weeks 34 to 48) has a lower water volume than the first season and reaches its maximum values between weeks 38 to 46.

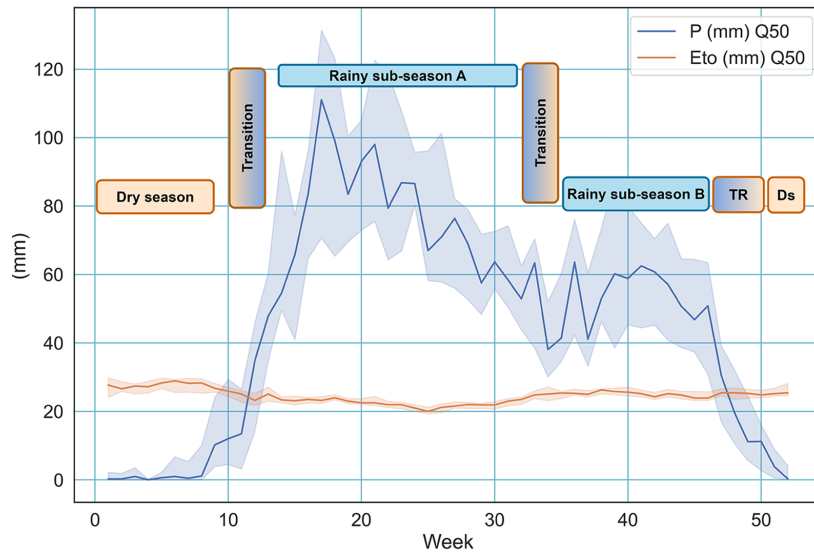


Figure 4. Weekly climatic balance and precipitation seasons (P – precipitation, Eto – reference evapotranspiration, Tr – transition, Ds – dry season)

The periods determining the change in rainfall quantity are known as transitional seasons and the proportion of precipitation during these periods varies according to the year (i.e., rainy years). Some periods mark the change between two seasons (i.e., from the dry to the wet season and vice versa) or between two sub-seasons, see Figure 3. The first transitional season occurs between weeks 9 to 13 and was associated with the approach of the ITCZ from southern latitudes (Leon et al., 2018) and the start of the rainy

season. A second transitional change occurs in the rainy sub-seasons between weeks 34 to 38, due to the displacement of the ITCZ toward the northern latitudes of the country and a subsequent return toward southern latitudes.

According to 50 years of historical series data, during week 13 the rainy season begins and is characterized by more precipitation than evapotranspiration. This period can sometimes be anticipated, as in 2004, 2006, and 2010, or delayed like in 2001, 2008, and 2015 (Figure

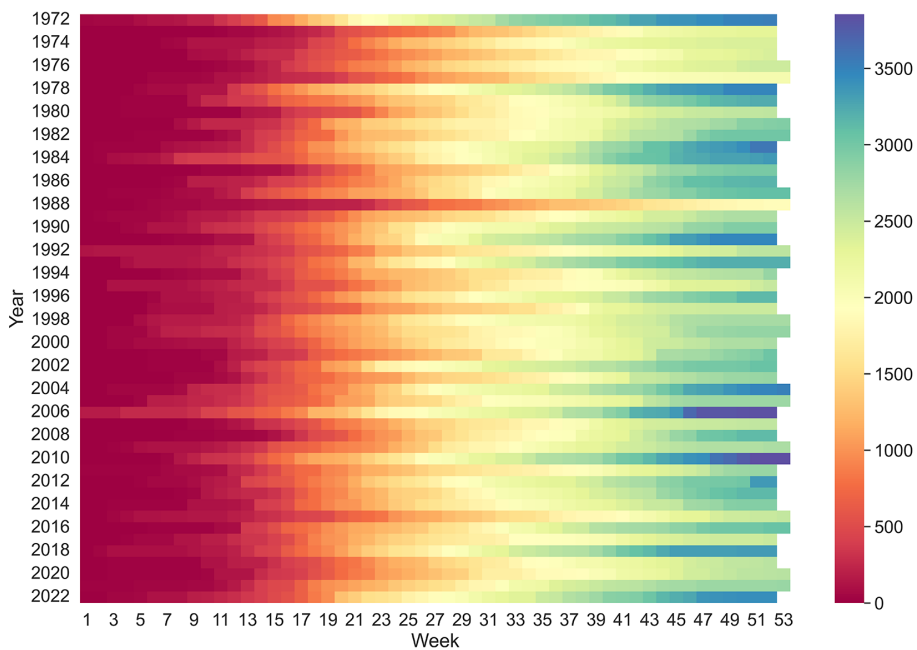


Figure 5. Accumulated annual precipitation on a weekly scale

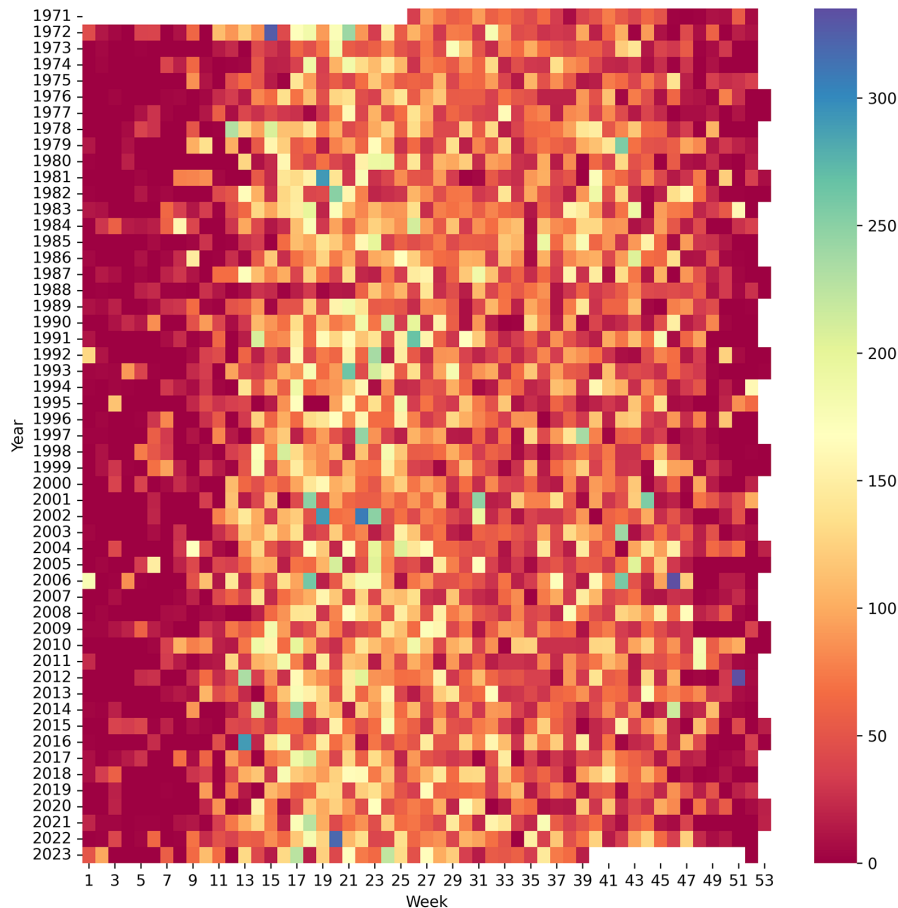


Figure 6. Weekly precipitation in historical series

4). The historical distribution of weekly rainfall shows that short periods without rainfall may occur during the rainy season, as well as isolated rains during the dry season, Figure 5.

The frequency of dry weeks during the rainy sub-season B (Figure 6) is notable. During sub-season B, soil water availability decreases, with water scarcity negatively impacting the phenological stages of annual crops (germination, flowering, and seedling filling) which are highly vulnerable to water deficits (Fahad et al., 2017).

Rainfall trends

The correlation analysis revealed non-auto-correlated and non-stationary behavior associated with annual precipitation and the annual number of rainy days. It provides evidence of oscillations within two years (Figure 7) in the annual precipitation plot and is confirmed by the strip with alternating positive and negative values for the annual rainfall series. However, the annual number of rainy days was found to have a ten-year oscillation period (Figure 7a and 7b).

The Mann–Kendall test did not identify significance in the annual precipitation trend as shown in Table 5. The series “Number of days with rain per year” showed ($p < 0.05$), with a decreasing precipitation trend.

The previous results (Table 5) illustrate a change in rainfall patterns. The trend has been negating with a reduction equivalent to 17 days of annual rain during the past 48 years (Figure 8). Sen’s estimated slope allowed the identification of the trend’s magnitude in the series “number of days with rain per year” with a value of 0.40.

The results indicate that annual precipitation values were maintained, but that the annual number of days with rainfall decreased between 1972 to 2021 (Table 5, Figure 8). The rainfall pattern described reveals an increase in rainfall intensity, and precipitation events increased from 14.8 to 16.2 mm/day over the 49-year period. The extreme (greater) rain values of the annual rainy days tend to appear with a 20-year frequency; and the minimum value frequencies occurred approximately 6, 26, and 46 years apart. Like annual precipitation, weekly precipitation did not

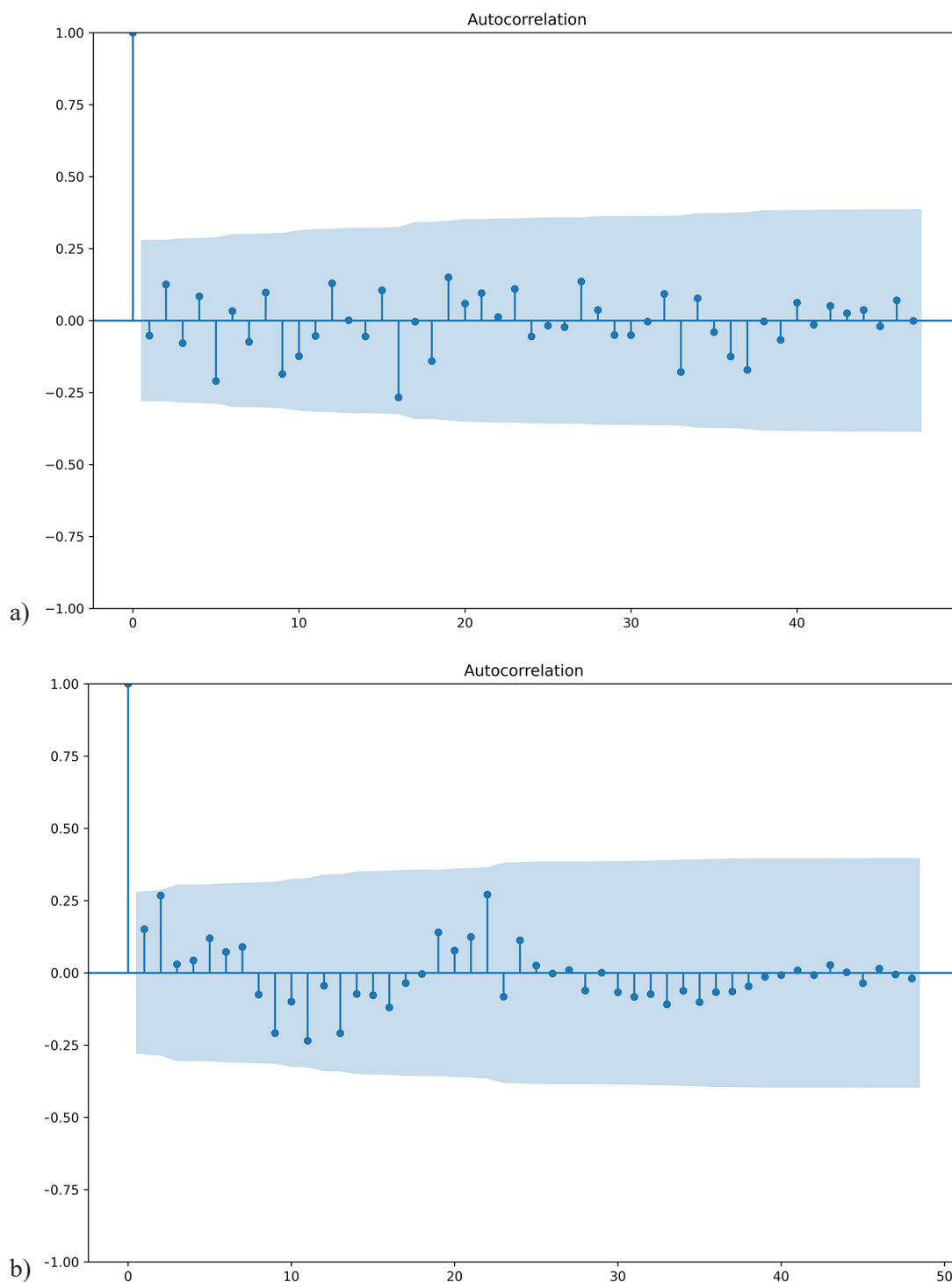


Figure 7. (a) Annual precipitation correlogram and (b) number of days with annual rain

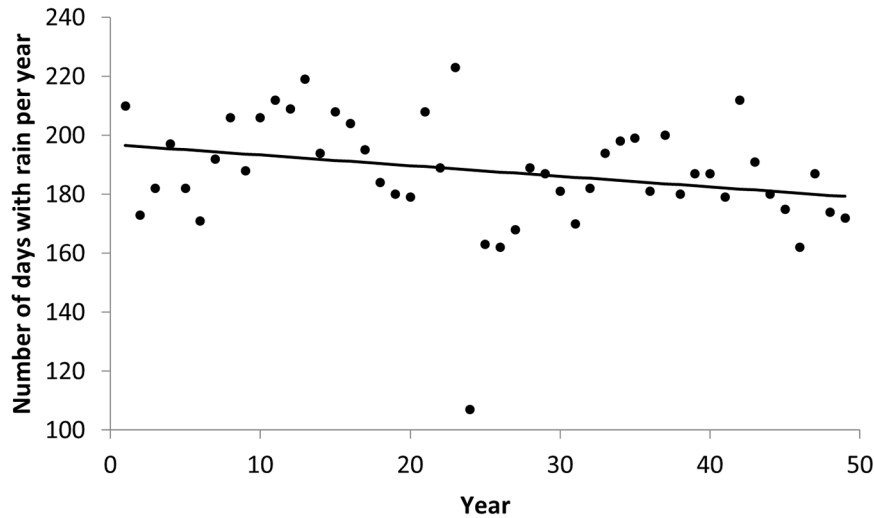
present autocorrelations as shown in Table 6. The Mann–Kendall test revealed significant trends in 5 of the 52 weeks annually. Three periods of the year revealed significant trends; the first was during the dry season in week 3 (January), the second was at the beginning of the rainy season during weeks 15, 19, and 20 (April), the third was during the end of the rainy season during week

45 (November). The analysis demonstrates a decreasing trend (i.e., becoming drier) during week 20 each year between 1972 to 2021. This was a form of weekly scale equilibrium, and this behavior was the opposite of the non-significance of the annual scale, as shown in Table 2. Nevertheless, despite the recurrence of dry periods during weeks 3, 15, 19, and 45; these weeks became

Table 5. Trends in annual precipitation and number of days with rain per year

MK test	P	Z	Earring	Trend
Annual rainfall	0.50	0.6637	3.03	None
Annual rainy days	0.01	-2.5103	0.40	Decreasing

Note: very significant, NS: not significant.

**Figure 8.** Trend of number of days with rain per year

wetter during the last 50 years (Table 6). The increasing trend during week 3 had positive effects on livestock systems. This positive effect was associated with water use during the dry season which allowed for the increase in the forage supply. The rainy-season-associated water increase could affect annual crops and pastures due to the greater frequency of soil saturation which affects the root development and production of plants and generates greater volumes of runoff and erosion (Mohamadi and Kavian, 2015). The trend of the number of days with rain on a weekly scale was significant in 9 of the 52 weeks of the year; with only 5 weeks evidencing autocorrelation, and the weeks between July and December showing a decreasing trend. This is shown in Table 7.

Within the annual series, the decreasing trend observed in the number of rainy days was ≤ 17 days during the second half of the year. This tendency increased the likelihood of drought affecting crops due to the low available water supply during this period. The modified MK test with pre-bleaching confirmed the significance of trends during weeks 35, 41, 47, and 49; with no significance for week 40. More detailed information can be found in Table 8. The trend of decreasing rainy days during weeks 33, 35, 38, and 49 evidenced the change in rainfall patterns which

reduced soil moisture availability and generated water stress and low crop yields.

Water supply dynamics

The first half of the year proved favorable for sowing annual crops under rainfed conditions due to high soil water availability. The rainfall during this part of the year (April to July) favored an optimal soil moisture condition with fluctuating FC values and sometimes experienced days with water deficits (with a maximum of 29 days). Detailed information is shown in Table 9. The weather conditions of the second half of the year (August to December) were unsuitable for the crop systems because they experienced 5 to 30 days of water deficits. This wide range of deficits generated uncertainty in the region. Despite this, the grasslands can support up to 36 days of water deficits with reduced biomass production. *Urochloa decumbens*, the most cultivated grass in the zone, is adapted to prolonged droughts, recovers very well, and protects the soil from rainfall (Beloni et al., 2018). The actual evapotranspiration values reflected water requirements per semi-annual cycle of between 265 to 400 mm (Table 10). The highest evapotranspiration values were observed in the grasslands, corn, and rice during

Table 6. Weekly precipitation trends (Traditional MK)

Week	Autocorrelation	Trend	P-value	Z-value
3	NO	Increasing	0.07**	1.80
15	NO	Increasing	0.10**	1.66
19	NO	Increasing	0.05*	1.92
20	NO	Decreasing	0.09**	-1.70
45	NO	Increasing	0.02*	2.32
Other weeks		NO	NS (> 0.1)	

Note: * very significant, ** significant, NS: not significant.

Table 7. Trends in number of days with weekly rain

Week	Autocorrelation	Trend	P-value	Z-value	Earring
3	NO	Increasing	0.08**	1.72	0.00
27	NO	Decreasing	0.03*	-2.11	0.00
33	NO	Decreasing	0.02*	-2.36	-0.02
35	YES	Decreasing	0.00*	-3.92	-0.04
38	NO	Decreasing	0.01*	-2.65	-0.04
40	YES	Decreasing	0.03*	-2.18	-0.02
41	YES	Increasing	0.08**	1.75	0.00
47	YES	Decreasing	0.07**	-1.81	0.00
49	YES	Decreasing	0.01*	-2.54	-0.04
Other weeks		NO	NS (> 0.1)		

Note: * significance of 0.05, ** significance of 0.1, NS: not significant.

Table 8. Modified MK test with prebleach

Week	Trend	P_value	Z_value	Earring
35	Decreasing	0.00*	-2,875	-0.04
40	NO	0.15	-1.44	-0.02
41	Growing	0.06**	1,854	0.05
47	Decreasing	0.02*	-2,270	0.00
49	Decreasing	0.07**	-1,826	-0.04

Note: * significance of 0.05, ** significance of 0.1, NS: not significant.

Table 9. Days with crop water deficit and excess during the years 2010, 2016 and 2020

Year	Crop	Semester A		Semester B	
		Deficit (days)	Excess (days)	Deficit (days)	Excess (days)
2010	Rice	12	53	15	3.4
	Soybean	0	52	5	38
	Corn	6	57	10	43
	Grass	17	66	20	49
2016	Rice	9	48	28	28
	Soybean	4	48	19	30
	Corn	2	54	21	28
	Grass	23	53	36	43
2020	Rice	12	42	30	25
	Soybean	4	48	15	25
	Corn	16	48	27	30
	Grass	29	61	36	31

Table 10. Crop deficits and excesses in productive cycle in millimeters

Year	Request crop water*	Semester A		Semester B	
		Deficit (mm)	Excess (mm)	Deficit (mm)	Excess (mm)
2010	Rice (342-374 mm)	27	1037	37	726
	Soybean (275-301 mm)	0	1039	17	605
	Corn (354-381 mm)	18	1092	3.4	803
	Grass (372-383 mm)	47	1361	45	976
2016	Rice (337-408 mm)	21	899	94	439
	Soybean (265-328 mm)	13	808	73	485
	Corn (345-383 mm)	3	909	85	451
	Grass (360-421 mm)	47	1047	116	654
2020	Rice (340-384 mm)	21	781	97	399
	Soybean (275-308 mm)	4	833	43	393
	Corn (354-395 mm)	24	806	78	410
	Grass (364-399 mm)	82	1076	123	448

Note: * hydric requirement of semester A and B.

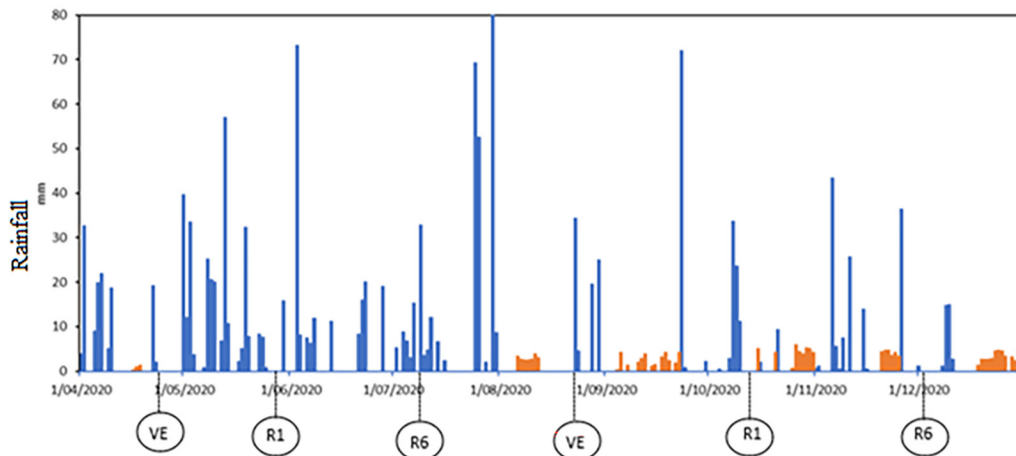
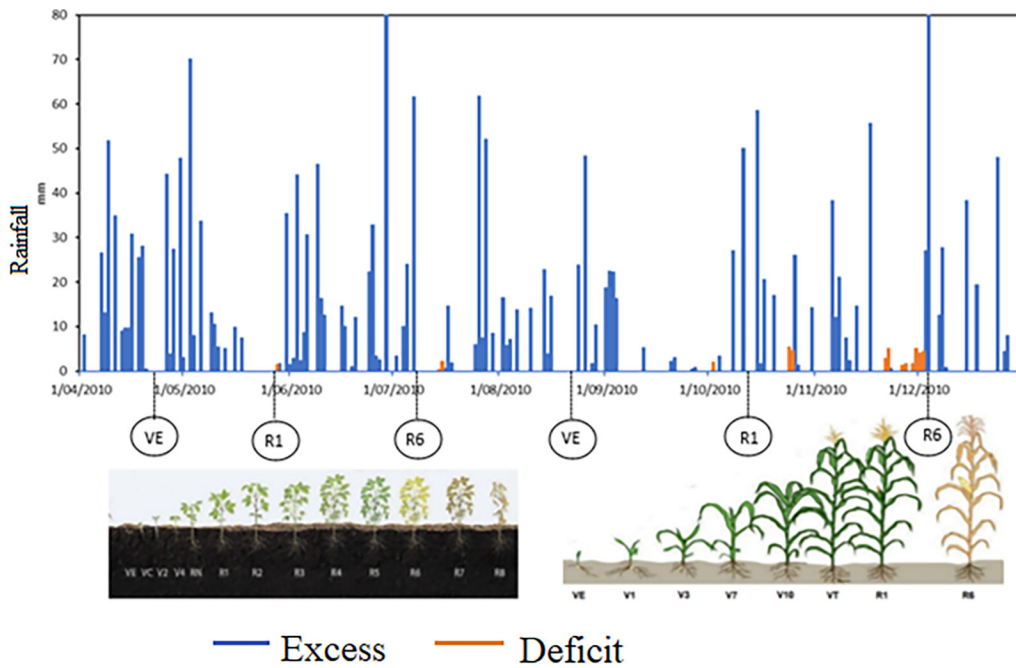


Figure 9. Agroclimatic balance in relation to the phenology of semi-annual crops in rotation during the years 2010 and 2020

the second half of the year. Detailed information is shown in Table 10. During the study period, the first semiannual period is noteworthy due to excessive water, with 781 to 1361 mm of rainfall.

The daily dynamics of the water supply associated with annual crops in semiannual rotation in the context of different phenological stages over two years were characterized by extreme annual precipitation and are illustrated in Figure 9. The year 2010 stands out as the year with the highest annual rainfall in the study series and resulted from the negative phase of ENSO. In 2010 there was a change in the rainfall distribution pattern, and this increased the water supply volume and number of rainy days during the crop cycle.

In comparison to historical values, 2020 had a different rainfall distribution pattern. Sub-season A experienced successive precipitation which generated soil water excesses, and sub-season B produced a soil water deficit, as shown in Figure 9. This alternation of rainfall excesses and deficits generates conditions unfavorable to achieving competitive crop yields. Studies report that soil water deficits during corn's vegetative stage (between emergence and flowering) affect production levels (Sah et al., 2020; Shao et al., 2021). Previous research has indicated that when two periods with water deficits occur between flowering (R1) and physiological maturity (R6), unfavorable conditions for grain formation generate low yields (Zhang et al., 2019). Short drought period was possible during the rainy season from August to December 2020. This is illustrated in Figure 9.

DISCUSSION

The spatial precipitation variability in the annual rainfall for the basin, decreased in the transect Villavicencio - Puerto Lopez (Bernal et al., 2013). This finding is related to wind direction, where topography influences convective activity (Poveda et al., 2020). The dry season was characterized by low rainfall and increased wind speeds, which are influenced by the low-level jet of the Orinoco phenomenon (Jiménez-Sánchez et al., 2019). The movement of clouds loaded with moisture rising toward the mountain are responsible for the most significant precipitation in the upper part of the basin (Poveda et al., 2020), and wind behavior explains the direction of windward convective rains. Standard deviation values revealed significant annual precipitation variations in the

extreme east of the basin, the effect of humidity toward the mountains, and the variation in precipitation affected by external topographical factors. Under these conditions, the threat of extreme precipitation increases. The observed precipitation variability of approximately 1000 mm (Figure 2) can be interpreted based on crop yields. Climatic factors explain 6% to 60% of space-time variability in rice crops yields in the departments of Meta and Tolima, Colombia (Delerce et al., 2016)

The results confirm that the evaluated ENSO indices do not define the interannual variability of rainfall in the study area, and do not always coincide with drought years associated with El Niño and La Niña (stormy years). Arango et al. (2015) reported similar results for the same analysis at the national scale, and these also proved unreliable in predicting precipitation patterns in the Orinoquía region based on the presence of the ENSO phenomenon. Other studies by Esquivel et al. (2018) found low predictability toward the Eastern Plains region (department of Casanare) using traditional indices. Esquivel et al. results suggested prioritizing research on this topic and considered improving the quality and density of the Orinoco basin's weather station network. The results to the present study differ from Colombian Andean research, where the ONI and BEST indices were adequate predictors of monthly precipitation with up to 3 months of delay, becoming a useful tool in the planning of coffee crops (Ramírez et al., 2018). Although it has been reported that ONI has a greater relationship with the anomalies signaled in other study area (Cali, Colombia), it is not necessarily the most accurate for signaling the Niño and Niña years of the ENSO phenomenon, it's probably due to the fact that this index is a macro-climatic order (Pérez-Ortiz et al., 2022)

Climatic analysis on a weekly scale reveals a monomodal rainfall regimen for the Colombian Orinoquía. This tends toward an intermediate or mixed regimen (Urrea et al., 2019). Additionally, decreasing rainfall between August and September is explained by the low influence of the ITCZ (Leon et al., 2018). During this period, trade winds from the southeast transport clouds from the Amazon basin to the Orinoquía, favoring the wettest conditions compared with those in the Andean zone (Espinoza et al., 2020; Ortega, 2021). Ultimately, the behavior of rainfall in the tropics tends to be unpredictable (Hartshorn, 2013). The results in this study show climatological analysis allows for defining the rainfall pattern

in equatorial zones on a weekly scale (Figure 4). The analysis will be used for land use planning based on the amount of water precipitation and crop demand according to their production cycles and phenology (Chica Ramirez et al., 2021).

The distribution of weekly rainfall in the historical record identifies intra-annual variability. This variability generates moments of water stress in crops (Osakabe et al., 2014) and the physical conditions of Orinoquía region soils aggravate this situation. The soil in the region has poor pore distribution characterized by a high proportion of micropores and low amounts of macro and mesopores. Given this situation, the implementation of agroforestry systems mitigates soil physical impacts, improving soil aggregation and porosity processes (Duran-Bautista et al., 2023). In the agricultural holdings in the amazon basin, the addition of organic matter, carbon inputs and management practices than residues incorporation, harvest past management combined with vegetation management providing abundant soil mulch and little soil disturbance, improvement soil physic hydrological properties, water availability, bulk density, soil porosity and root developed (de Oliveira et al., 2022; Reichert et al., 2016). Other authors recommend improving the production capacity of the soil than; a strategy to increase soil water retention (Gallo et al., 2013). It's necessary considering the periodic monitoring of ecosystem services indicators, for make the management decisions in local level to maintain and preserve the balance of production systems (Moreno-Conn et al., 2022).

The “annual precipitation” in this study displayed no trend, but other studies have suggested a slight increase in Orinoquía region precipitation related to climate change (Hurtado and Mesa, 2016). in the other way, Arrieta-Pastrana et al. (2023), using the same data source found that the annual precipitation series were homogeneous and with no significant trend. In the series consisting of the annual number of rainy days, this study finds very significant results with a decreasing trend (Figure 8).

The Annual rainy days trends (Table 5 and Figure 8), found in this work, agree with the RCP 4.5 climate change scenarios for the year 2040, reported in the Regional Comprehensive Climate Change Plan for the Orinoquía region - PRICCO (2017a) and the global and regional climate change report (IPCC, 2022). It is important to mention that the results obtained in this study and PRICCO show with a low level of certainty,

the increase in annual precipitation. However, according to the results described in Table 5, the drastic changes in precipitation are given by the trend of reduction in the number of rainy days per year. This reduction is associated with two threatening factors for agricultural production, the increase in the intensity of rainfall events and the reduction of precipitation in the transition season from rainy to dry periods (October – November) (Table 7), as reported in Arias et al (2021). The weather in the basin showed variations approximately every 10 years (Figure 8), coinciding with reports of the influences of decadal climatic phenomena by IDEAM and UNAL (2018).

Results applying global climate models (GCM) from CMIP5, A negative signal with respect to changes in precipitation, evapotranspiration, and runoff is observed on most of the continent. Consequently, important decreases in the average annual discharge are expected for the Orinoco basin, which would be around 8–14% at least – RCP4.5 and RCP8.5, respectively (Brêda et al., 2020). It is important to emphasize that the global climate models of the CMIP5 and CMIP6 generation have difficulty in representing the Intertropical Convergence Zone (B. Tian and Dong, 2020), the main determinant of intra-annual rainfall behavior, as well as rain formation processes associated with the drastic change in relief (Sierra et al., 2015), as is the case of the zones of the eastern plains located in the piedmont. As reported by Littmann (2008) surface properties such as aspect, slope angle, surface albedo and roughness determine boundary conditions for specific micro and topoclimates which, in turn, will counteract on the associated micro-habitats. On the other hand, the spatial and temporal resolution of global models, the main determinants of the intra-annual behavior of climate elements at the time of generating future scenarios, do not allow a fair comparison with the local analysis (weekly scale) performed in this study (Figure 4 and 5).

The observed weekly precipitation tendency coincides with forecast reports for the comprehensive regional climate change plan in the Orinoquía region (PRICCO 2017) , report precipitation increases during the dry season (December to January) and slight increases during the rainiest months (May to August), researchs about tends sub – monthly are not available in this zone, and the monthly results have less seasonal variability than weekly (Torres-Pineda and Pabón-Caicedo, 2017). The growth trend during week 3 had positive

effects on the livestock systems associated with the use of water in the dry season and allows it to increase the forage supply. The soil water increases during the rainy season were found to negatively impact in annual crops and grasslands, and the frequency of saturated soils in the last years affected the root development and production of plants, thereby generating more runoff and soil erosion.

The decreasing trends of rainy days in weeks 33, 35, 38, and 49 (second half of the year) were related to the changes in rainfall patterns evidenced by changes in soil moisture (e.g., drought). These resulted in consequences for soil-mediated processes (Robinson et al., 2016) and generated water stress and low crop yields. Drought was one of the causes of the decrease in the planted area during the second half period in the Orinoquía region (PRICCO 2017)

Water supply analyses showed excess water (781–1361 mm) during the first half of the year (April to July). This response was associated with soil nature characterized by low infiltration capacity (Rivera and Amézquita, 2013) which generated surface runoff and waterlogging in poorly drained soils. Research by Rhine et al., (2010) indicated that soybean crop yields were affected by soil water saturation for several consecutive days. In Colombian Orinoquía soils, the same action has been observed under high humidity conditions, affecting the effectiveness of nitrogen-fixing bacteria, delaying the crop cycle, and necessitating additional nitrogen applications.

During the second half of the year (August to December), short periods of water deficit occur and are defined as an agricultural drought (Tian et al., 2022). This refers to an abnormal drop in rainfall during the suitable crop growth period. These conditions have been analyzed in the country at a 1:9,000,000 scale and identify meteorological and agricultural drought as a major problem in the Colombian agricultural sector. The IDEAM study revealed the presence of droughts intervals during the rainy season, especially during the second semiannual crop period in the Orinoquía region (August to December). Research estimated water consumption for soybean at 4.5 mm/day (Anda et al., 2020); thus, exhausting soil water reserves in 4 days is making necessary to use irrigation systems to guarantee production. These results revealed 20 days of soil drought conditions, so, during this period, soil requires additional irrigation, especially during the eight critical weeks of the 2020b cycle. The savanna grasslands'

advantage its adaptability to extreme drought and wet conditions in the soils because the genotypes temporarily tolerate the extreme conditions (Zi et al., 2023). The frequency or amplitude of extreme events reduces forage supply, but the 2010 rainy season increased the productivity of forage crops and grasslands (Beloni et al., 2018).

CONCLUSIONS

ENSO was found to have no effect on annual rainfall within the study catchment area. The correlation between ENSO periods and changes in weather conditions was found to be an inappropriate parameter for use as a tool for agricultural planning in the study zone.

The use of weekly analysis for crop water supplies allowed the identification of an intermediate rainfall regime occurring between monomodal and bimodal, giving a realistic scenario of precipitation dynamics during the rainy season at the Orinoquía savanna sub-basins scale. This research demonstrates the importance of meteorological information as an instrument to properly plan for planting season production. The decrease in annual rainy days indicates variations in the frequency and intensity of precipitation, increasing the probability of both extreme drought and wet events influencing water supply variability for crops in the sub-basin. This trend is higher during the second half of the year. Short dry periods during the rainy season or isolated rains during the dry season affect water management at the individual farmer level as well as irrigation usage.

Intra-annual variability of precipitation in the sub-basin shows a high-water supply (i.e., water excess) during the rainy sub-season of April to July, but from August to November (i.e., second rainy sub-season), rainfall more often reduces the risk of soil moisture deficits. The present scenario prioritizes the implementation of water availability strategies associated with climate change or rainfall changes, supported by meteorological and soil moisture information at the individual farm level.

The implementation of a meteorological network in the Llanos Orientales piedmont sub-basins (similar to the Caño Quenane sub-basin) using rainfall gauges separated by 11 km allows the identification of the spatial variability of annual precipitation, thus reducing the climatological risk for farmers and growers. This information is

relevant for decision-makers at the Orinoquía region level and diminishes the risk associated with drought periods. For the future research is convenient to use permanent meteorological instrumentation and the comparison with other methodologies such as ERA5 and ERA5-Land Reanalysis, CMIP5, CMIP6 and CORDEX climatological projections, CHIRPS database, IMERG data. General Circulation Models (GCM), Coupled Models.

Acknowledgments

This work was possible thanks to the project ID 1000414 “Improvement of the productive capacity of the soil to contribute to the increase in the competitiveness and sustainability of transitional crops in the Flat High Plains and plain piedmont, under climate change scenarios” of the Corporación Colombiana de Investigación Agropecuaria (AGROSAVIA), and the master thesis “Estimation of water supply for crop planning in a hydrographic basin of the Colombian Orinoquía, from Universidad Nacional de Colombia – Agronomy faculty. The financial support 2023–2024 for style correction of research papers in English, Facultad de Minas, Universidad Nacional de Colombia Sede Medellín - Hermes code 59910. Thanks to Kiora V from Enago for the language and grammar edition.

REFERENCES

- Alan, A.T.M., Rahman, M.S., Sadaat, A.H.M. (2014). Markov Chain Analysis of Weekly Rainfall Data for Predicting Agricultural Drought. In *Computational Intelligence Techniques in Earth and Environmental Sciences*, 109–128. https://doi.org/https://doi.org/10.1007/978-94-017-8642-3_6
- Allen, R.G., Pereira, L.S., Raes, D., Smith, M. (1998). Crop evapotranspiration, Guides for determining crop water requirements. (Evapotranspiración del cultivo, Guías para la determinación de los requerimientos de agua de los cultivos). FAO - Food and Agriculture Organization of the United Nations, 56. <https://www.fao.org/3/x0490s/x0490s.pdf>
- Anda, A., Simon, B., Soos, G., Teixeira da Silva, J.A., Farkas, Z., Menyhart, L. (2020). Assessment of Soybean Evapotranspiration and Controlled Water Stress Using Traditional and Converted Evapotranspirometers. *Atmosphere*, 11(8), 830. <https://doi.org/10.3390/atmos11080830>
- Arias, P.A., Ortega, G., Villegas, L. D., Martínez, J.A. (2021). Colombian climatology in CMIP5/CMIP6 models: Persistent biases and improvements. *Revista Facultad de Ingeniería Universidad de Antioquia*. <https://doi.org/10.17533/udea.redin.20210525>
- Armenteras, D., Meza, M. C., González, T. M., Oliveras, I., Balch, J. K., Retana, J. (2021). Fire threatens the diversity and structure of tropical gallery forests. *Ecosphere*, 12(1). <https://doi.org/10.1002/ecs2.3347>
- Arrieta-Pastrana, A., Saba, M., Puello Alcázar, A. (2023). Analysis of Climate Variability and Climate Change in Sub-Daily Maximum Intensities: A Case Study in Cartagena, Colombia. *Atmosphere*, 14(1), 146. <https://doi.org/10.3390/atmos14010146>
- Attanasio, A., Pasini, A., Triacca, U. (2013). Granger Causality Analyses for Climatic Attribution. *Atmospheric and Climate Sciences*, 3(4), 515–522. <https://doi.org/10.4236/acs.2013.34054>
- Beloni, T., Santos, P.M., Rovadoscki, G.A., Balachowski, J., Volaire, F. (2018). Large variability in drought survival among *Urochloa* spp. cultivars. *Grass and Forage Science*, 73(4), 947–957. <https://doi.org/10.1111/gfs.12380>
- Bera, B., Shit, P.K., Sengupta, N., Saha, S., Bhattacharjee, S. (2021). Trends and variability of drought in the extended part of Chhota Nagpur plateau (Singbhum Protocontinent), India applying SPI and SPEI indices. *Environmental Challenges*, 5(September), 100310. <https://doi.org/10.1016/j.envc.2021.100310>
- Bernal, J., Peña, A., Díaz, N., Obando, D. (2013). Climatic conditions of the Colombian flat plateau in the context of climate change (Condiciones climáticas de la altillanura plana colombiana en el contexto de cambio climático). In E. Amézquita, I. Rao, M. Rivera, I. Corrales, J. Bernal (Eds.), *Sistemas agropastoriles: Un enfoque integrado para el manejo sostenible de oxisoles de los Llanos Orientales de Colombia*. Centro Internacional de Agricultura Tropical (CIAT) Ministerio de Agricultura y Desarrollo Rural (MADR) Corporación Colombiana de, 14–28.
- Brêda, J.P.L.F., de Paiva, R.C.D., Collischon, W., Bravo, J.M., Siqueira, V.A., Steinke, E.B. (2020). Climate change impacts on South American water balance from a continental-scale hydrological model driven by CMIP5 projections. *Climatic Change*, 159(4), 503–522. <https://doi.org/10.1007/s10584-020-02667-9>
- Bustamante, C. (2019). *Great Book of the Colombian Orinoquia (Gran Libro de la Orinoquia Colombiana)*. Instituto de Investigación de Recursos Biológicos Alexander von Humboldt-Deutsche Gesellschaft für Internationale Zusammenarbeit (GIZ) GmbH. <http://repository.humboldt.org.co/handle/20.500.11761/35408>
- Chica, H., Quiñones, A.J.P., Jiménez, J.F.G., Bonilla, D.O., Herrera, N.M.R. (2014). *SueMulador: Tool*

- for the Simulation of Missing Data in Daily Climate Series of Equatorial Zones. *Revista Facultad Nacional de Agronomía Medellín*, 67(2), 7365–7373. <https://doi.org/10.15446/rfnam.v67n2.44179>
14. Chica Ramirez, H.A., Gómez Gil, L.F., Bravo Bastidas, J.J., Carbonell González, J.A., Peña Quiñones, A.J. (2021). Site-specific intra-annual rainfall patterns: a tool for agricultural planning in the Colombian sugarcane production zone. *Theoretical and Applied Climatology*, 146(1–2), 543–554. <https://doi.org/10.1007/s00704-021-03755-1>
 15. Chisanga, C.B., Nkonde, E., Phiri, E., Mubanga, K.H., Lwando, C. (2023). Trend analysis of rainfall from 1981–2022 over Zambia. *Heliyon*, 9(11), e22345. <https://doi.org/10.1016/j.heliyon.2023.e22345>
 16. Cui, X. (2020). Climate change and adaptation in agriculture: Evidence from US cropping patterns. *Journal of Environmental Economics and Management*, 101, 102306. <https://doi.org/10.1016/j.jeem.2020.102306>
 17. da Silva, E.H.F.M., Gonçalves, A.O., Pereira, R.A., Fattori Júnior, I.M., Sobenko, L.R., Marin, F.R. (2019). Soybean irrigation requirements and canopy-atmosphere coupling in Southern Brazil. *Agricultural Water Management*, 218(October 2018), 1–7. <https://doi.org/10.1016/j.agwat.2019.03.003>
 18. Das, D.P., Kothari, K., Pandey, A. (2024). Comprehensive analysis of spatiotemporal variability of rainfall-based extremes and their implications on agriculture in the Upper Ganga Command Area. *Environmental Monitoring and Assessment*, 196(2), 111. <https://doi.org/10.1007/s10661-023-12265-8>
 19. Dastane, N.G. (1978). Effective rainfall in irrigated agriculture. *FAO Irrigation and Drainage Engineering*, 4(1), 25. <https://www.fao.org/3/X5560E/X5560E00.htm>
 20. de Boer-Euser, T., McMillan, H.K., Hrachowitz, M., Winsemius, H.C., Savenije, H.H.G. (2016). Influence of soil and climate on root zone storage capacity. *Water Resources Research*, 52(3), 2009–2024. <https://doi.org/10.1002/2015WR018115>
 21. de Oliveira, R.L.L., Vasconcelos, S.S., Teixeira, W.G., Viana-Junior, A.B., Castellani, D.C., Kato, O.R. (2022). Management Practices Affect Soil Carbon and Physical Quality in Oil Palm Agroforestry Systems in the Amazon. *Journal of Soil Science and Plant Nutrition*, 22(4), 4653–4668. <https://doi.org/10.1007/s42729-022-00947-0>
 22. de Oliveira-Júnior, J.F., Mendes, D., Luiz, F.C.F.W., da Silva Junior, C.A., de Gois, G., da Rosa Ferraz Jardim, A.M., da Silva, M.V., Lyra, G.B., Teodoro, P.E., Pimentel, L.C.G., Lima, M., de Barros Sant, D., Rogelio, J.P. (2021). Fire foci in South America: Impact and causes, fire hazard and future scenarios José. *Journal of South American Earth Sciences*, 144(89), 2669. <https://doi.org/10.1016/j.jsames.2021.103623>
 23. Delerce, S., Dorado, H., Grillon, A., Rebolledo, M.C., Prager, S.D., Patiño, V.H., Varón, G.G., Jiménez, D. (2016). Assessing weather-yield relationships in rice at local scale using data mining approaches. *PLoS ONE*, 11(8). <https://doi.org/10.1371/journal.pone.0161620>
 24. Duran-Bautista, E.H., Angel-Sanchez, Y.K., Bermúdez, M.F., Suárez, J.C. (2023). Agroforestry systems generate changes in soil macrofauna and soil physical quality relationship in the northwestern Colombian Amazon. *Agroforestry Systems*, 97(5), 927–938. <https://doi.org/10.1007/s10457-023-00838-y>
 25. Egerer, S., Cotera, R.V., Celliers, L., Costa, M.M. (2021). A leverage points analysis of a qualitative system dynamics model for climate change adaptation in agriculture. *Agricultural Systems*, 189(February 2020). <https://doi.org/10.1016/j.agsy.2021.103052>
 26. Espinoza, J.C., Garreaud, R., Poveda, G., Arias, P.A., Molina-Carpio, J., Masiokas, M., Viale, M., Scaff, L. (2020). Hydroclimate of the Andes Part I: Main Climatic Features. *Frontiers in Earth Science*, 8(March), 1–20. <https://doi.org/10.3389/feart.2020.00064>
 27. Esquivel, A., Llanos-Herrera, L., Agudelo, D., Prager, S.D., Fernandes, K., Rojas, A., Valencia, J.J., Ramirez-Villegas, J. (2018). Predictability of seasonal precipitation across major crop growing areas in Colombia. *Climate Services*, 12(September), 36–47. <https://doi.org/10.1016/j.cliser.2018.09.001>
 28. Fahad, S., Bajwa, A.A., Nazir, U., Anjum, S.A., Farooq, A., Zohaib, A., Sadia, S., Nasim, W., Adkins, S., Saud, S., Ihsan, M. Z., Alharby, H., Wu, C., Wang, D., Huang, J. (2017). Crop production under drought and heat stress: Plant responses and management options. In *Frontiers in Plant Science* (8). Frontiers Media S.A. <https://doi.org/10.3389/fpls.2017.01147>
 29. Fontanilla-Díaz, C.A., Preckel, P.V., Lowenberg-DeBoer, J., Sanders, J., Peña-Lévano, L.M. (2021). Identifying profitable activities on the frontier: The Altillanura of Colombia. *Agricultural Systems*, 192(May). <https://doi.org/10.1016/j.agsy.2021.103199>
 30. Gallo, O., Bernal, J., Baquero, J., Botero, R., Gómez, J. (2013). Effect of Three Systems of Incorporation of Dolomite Limestone in the Colombian Flat Plains. *Suelos Ecuatoriales Sociedad Colombiana de La Ciencia Del Suelo*, 43(1), 24–28.
 31. Galvis Quintero, J.H., Anaya, O.C., Bernal Riobo, J.H., Baquero, J.E. (2018). Evaluation of structural stability and pore space in a savanna Oxisol from the Eastern Plains of Colombia (Evaluación de la estabilidad estructural y espacio poroso en un Oxisol de sabana de los Llanos Orientales de

- Colombia). *Journal of Physical Therapy Science*, 9(1), 1–11. <http://dx.doi.org/10.1016/j.neuropsychologia.2015.07.010><http://dx.doi.org/10.1016/j.visres.2014.07.001><https://doi.org/10.1016/j.humov.2018.08.006><http://www.ncbi.nlm.nih.gov/pubmed/24582474><https://doi.org/10.1016/j.gaitpost.2018.12.007>
32. Gao, F., Wang, Y., Chen, X., Yang, W. (2020). Trend analysis of rainfall time series in Shanxi province, Northern China (1957-2019). *Water (Switzerland)*, 12(9), 1–22. <https://doi.org/10.3390/W12092335>
 33. Hartshorn, G.S. (2013). Tropical Forest Ecosystems. In *Encyclopedia of Biodiversity: Second Edition* 7(269–276). <https://doi.org/10.1016/B978-0-12-384719-5.00146-5>
 34. Hébert-Dufresne, L., Pellegrini, A.F.A., Bhat, U., Redner, S., Pacala, S.W., Berdahl, A.M. (2018). Edge fires drive the shape and stability of tropical forests. *Ecology Letters*, 21(6), 794–803. <https://doi.org/10.1111/ele.12942>
 35. Hoogenboom, G. (2000). Contribution of agrometeorology to the simulation of crop production and its applications. *Agricultural and Forest Meteorology*, 103(1–2), 137–157. [https://doi.org/10.1016/S0168-1923\(00\)00108-8](https://doi.org/10.1016/S0168-1923(00)00108-8)
 36. Hoyos, N., Escobar, J., Restrepo, J.C., Arango, A.M., Ortiz, J.C. (2013). Impact of the 2010-2011 La Niña phenomenon in Colombia, South America: The human toll of an extreme weather event. *Applied Geography*, 39(September 2011), 16–25. <https://doi.org/10.1016/j.apgeog.2012.11.018>
 37. Hurtado, A., Mesa, Ó. (2016). Climate change and space-time variability of precipitation in Colombia. *Revista EIA*, 12(574), 131–150.
 38. Ibrahim, M.A., Johansson, M. (2021). Attitudes to climate change adaptation in agriculture – A case study of Öland, Sweden. *Journal of Rural Studies*, 86(March), 1–15. <https://doi.org/10.1016/j.jrurstud.2021.05.024>
 39. IDEAM, UNAL. (2018). Climate variability and climate change in Colombia (Variabilidad climática y el cambio climático en Colombia) [Archivo PDF]. In Instituto de Hidrología, Meteorología y Estudios Ambientales – IDEAM Universidad Nacional de Colombia – UNAL (28). <http://documentacion.ideam.gov.co/openbiblio/bvirtual/023778/variabilidad.pdf>
 40. IPCC. (2020). Climate change and the earth (El cambio climático y la tierra). In Grupo Intergubernamental de Expertos sobre el Cambio Climático. https://www.ipcc.ch/site/assets/uploads/sites/4/2020/06/SRCCL_SPM_es.pdf
 41. IPCC. (2022). Global to Regional Atlas. In Pörtner, H.O., A. Alegría, V. Möller, E.S. Poloczanska, K. Mintenbeck, S. Götze (Eds.), *Climate Change 2022 – Impacts, Adaptation and Vulnerability* (2811–2896). Cambridge University Press. <https://doi.org/10.1017/9781009325844.028>
 42. Jiménez-Sánchez, G., Markowski, P.M., Jewtoukoff, V., Young, G.S., Stensrud, D.J. (2019). The Orinoco Low-Level Jet An Investigation of Its Characteristics and Evolution.pdf. *Journal of Geophysical Research: Atmospheres*, 124(10), 610–696, 711. <https://doi.org/https://doi.org/10.1029/2019JD030934>
 43. Leon, G., Arcila, A., Pulido, L.A., Kondo, T. (2018). Capítulo 25 Contenido Cambio climático y control biológico de insectos: visión y perspectiva de la situación Chapter 25 Climate change and biological control of insects: current situation and perspectives. In *Control biológico de fitopatógenos, insectos y ácaros* (Issue October, 572).
 44. Littmann, T. (2008). Topoclimate and Microclimate, 175–182. https://doi.org/10.1007/978-3-540-75498-5_12
 45. López, J.J., Goñi, M., San Martín, I., Erro, J. (2019). Análisis regional de frecuencias de las precipitaciones diarias extremas en Navarra. *Elaboración de los mapas de cuantiles. Ingeniería Del Agua*, 23(1), 33. <https://doi.org/10.4995/ia.2019.10058>
 46. Lozano, E. (2014). Eastern Plains Basin Compilation (Compilación de la cuenca de los Llanos Orientales). *Servicio Geológico Colombiano*, 1(Diciembre), 5–9.
 47. Mahlengule Zwane, E. (2019). Capacity Development for Scaling Up Climate-Smart Agriculture Innovations. In *Climate Change and Agriculture. IntechOpen*. <https://doi.org/10.5772/intechopen.84405>
 48. Mesri, M., Ghilane, A., Bachari, N.E.I. (2013). An approach to spatio-temporal analysis for climatic data. *Revue Des Energies Renouvelables*, 16, 413–424.
 49. Mohamadi, M.A., Kavian, A. (2015). Effects of rainfall patterns on runoff and soil erosion in field plots. *International Soil and Water Conservation Research*, 3(4), 273–281. <https://doi.org/10.1016/j.iswcr.2015.10.001>
 50. Moreno-Conn, L.M., Rodríguez-Hernandez, N.S., Arguello, J.O., Gallo Gordillo, O., Bernal-Riobo, J.H., Arango, M., Baquero, J.E. (2022). Land use change and its effect on ecosystem services in an Oxisol of the eastern High Plains of meta department in Colombia. *Frontiers in Environmental Science*, 10. <https://doi.org/10.3389/fenvs.2022.687804>
 51. Ortega, J.M.S. (2021). Evaluation of the transport of atmospheric moisture from the Atlantic Ocean to the Orinoco and northern Amazon basins during 2010 using the WRF-Tracers model (Evaluación del transporte de humedad atmosférica desde el océano Atlántico hacia las cuencas del Orinoco y el norte del Amazonas durante el año 2010 mediante el modelo WRF-Tracers) [Tesis de Ingeniería Ambiental]. In Universidad de Antioquia. https://biblioteca-digital.udea.edu.co/bitstream/10495/19697/1/SanchezJuan_2021_EvaluacionTransporteHumedad.pdf

52. Osakabe, Y., Osakabe, K., Shinozaki, K., Tran, L.S.P. (2014). Response of plants to water stress. *Frontiers in Plant Science*, 5(MAR), 1–8. <https://doi.org/10.3389/fpls.2014.00086>
53. Pardo, O., Torres, H., Trujillo, G., Trujillo, J. (2020). Impacts of climate change on the yields of Rice (*Oryza sativa* L) in the Llanos area, Colombia (Impactos del cambio climático sobre los rendimientos del Arroz (*Oryza sativa* L) en la zona llanos, Colombia). *AGLALA* ISSN 2215-7360, 11(2), 94–106. <https://revistas.curn.edu.co/index.php/aglala/article/view/1698>
54. Pathak, H. (2023). Impact, adaptation, and mitigation of climate change in Indian agriculture. *Environmental Monitoring and Assessment*, 195(1). <https://doi.org/10.1007/s10661-022-10537-3>
55. Andrés J Peña Q., Álvaro Jaramillo R., María J Paternina Q (2011). Detecting low frequency cycles in rainfall series from Colombian coffee-growing area by using descriptive methods. *Earth Sciences Research Journal*, 15(2), 109–114.
56. Pérez-Ortiz, M. A., Montenegro-Murillo, D.D., Vargas-Franco, V. (2022). Analysis of the influence of climatic variability on precipitation in the Cali River basin, Colombia (in Spanish). *DYNA*, 89(221), 168–177. <https://doi.org/10.15446/dyna.v89n221.101607>
57. Poveda, G., Espinoza, J.C., Zuluaga, M.D., Solomon, S.A., Garreaud, R., van Oevelen, P.J. (2020). High Impact Weather Events in the Andes. *Frontiers in Earth Science*, 8(May), 1–32. <https://doi.org/10.3389/feart.2020.00162>
58. Praveen, B., Talukdar, S., Shahfahad, Mahato, S., Mondal, J., Sharma, P., Islam, A. R. M. T., Rahman, A. (2020). Analyzing trend and forecasting of rainfall changes in India using non-parametrical and machine learning approaches. *Scientific Reports*, 10(1), 1–21. <https://doi.org/10.1038/s41598-020-67228-7>
59. PRICCO. (2017). Comprehensive Regional Climate Change Plan for the Orinoquía (in Spanish). Centro Internacional de Agricultura Tropical (CIAT), Cali, Colombia., No. 438.
60. Qiu, J., Shen, Z., Xie, H. (2023). Drought impacts on hydrology and water quality under climate change. *Science of The Total Environment*, 858, 159854. <https://doi.org/https://doi.org/10.1016/j.scitotenv.2022.159854>
61. Ramirez, C., Vélez U., J.J., Peña Q., A.J. (2018). Analyzing climatic indices to predict monthly rainfall in an agricultural region of the northern Andes (Caldas, Colombia) (in Spanish). *Investigaciones Geográficas*, 55, 111–126. <https://doi.org/10.5354/0719-5370.2018.48460>
62. Ramirez-Contreras, N.E., Fontanilla-Díaz, C.A., Pardo, L.E., Delgado, T., Munar-Florez, D., Wicke, B., Ruiz-Delgado, J., van der Hilst, F., Garcia-Núñez, J.A., Mosquera-Montoya, M., Faaij, A.P.C. (2022). Integral analysis of environmental and economic performance of combined agricultural intensification and bioenergy production in the Orinoquia region. *Journal of Environmental Management*, 303, 114137. <https://doi.org/10.1016/j.jenvman.2021.114137>
63. Reichert, J.M., Rodrigues, M.F., Bervald, C.M.P., Kato, O.R. (2016). Fire-Free Fallow Management by Mechanized Chopping of Biomass for Sustainable Agriculture in Eastern Amazon: Effects on Soil Compactness, Porosity, and Water Retention and Availability. *Land Degradation and Development*, 27(5), 1403–1412. <https://doi.org/10.1002/ldr.2395>
64. Rhine, M.D., Stevens, G., Shannon, G., Wrather, A., Sleper, D. (2010). Yield and nutritional responses to waterlogging of soybean cultivars. *Irrigation Science*, 28(2), 135–142. <https://doi.org/10.1007/s00271-009-0168-x>
65. Rivera, M., Amézquita, E. (2013). Biophysical characterization of monoculture and rotation systems in oxisols of the Eastern Plains of Colombia (Caracterización biofísica de sistemas en monocultivo y en rotación en oxisoles de los Llanos Orientales de Colombia). In E. Amézquita, I. Rao, M. Rivera, I. Corrales, J. Bernal (Eds.), *Sistemas agropastoriles : Un enfoque integrado para el manejo sostenible de oxisoles de los Llanos Orientales de Colombia* .. Centro Internacional de Agricultura Tropical (CIAT) Ministerio de Agricultura y Desarrollo Rural (MADR) Corporación Colombiana de (pp. 69–86). <http://hdl.handle.net/20.500.12324/35788>
66. Robinson, D.A., Jones, S.B., Lebron, I., Reinsch, S., Domínguez, M.T., Smith, A.R., Jones, D.L., Marshall, M.R., Emmett, B.A. (2016). Experimental evidence for drought induced alternative stable states of soil moisture. *Scientific Reports*, 6(September 2015), 1–6. <https://doi.org/10.1038/srep20018>
67. Ross, K. (2016). Preparing for an uncertain future with climate smart agriculture. *California Agriculture*, 70(1), 4–5. <https://doi.org/10.3733/ca.v070n01p4>
68. Sah, R.P., Chakraborty, M., Prasad, K., Pandit, M., Tudu, V.K., Chakravarty, M.K., Narayan, S.C., Rana, M., Moharana, D. (2020). Impact of water deficit stress in maize: Phenology and yield components. *Scientific Reports*, 10(1). <https://doi.org/10.1038/s41598-020-59689-7>
69. Shao, R., Jia, S., Tang, Y., Zhang, J., Li, H., Li, L., Chen, J., Guo, J., Wang, H., Yang, Q., Wang, Y., Liu, T., Zhao, X. (2021). Soil water deficit suppresses development of maize ear by altering metabolism and photosynthesis. *Environmental and Experimental Botany*, 192. <https://doi.org/10.1016/j.envexpbot.2021.104651>
70. Sierra, J.P., Arias, P.A., Vieira, S.C. (2015). Precipitation over Northern South America and Its

- Seasonal Variability as Simulated by the CMIP5 Models. *Advances in Meteorology*, 2015, 1–22. <https://doi.org/10.1155/2015/634720>
71. Soil Survey Staff. (2022). *Keys to Soil Taxonomy* (USDA Natural Resources Conservation Service, Ed.; 13th edition).
 72. Tian, B., Dong, X. (2020). The Double-ITCZ Bias in CMIP3, CMIP5, and CMIP6 Models Based on Annual Mean Precipitation. *Geophysical Research Letters*, 47(8). <https://doi.org/10.1029/2020GL087232>
 73. Tian, Q., Lu, J., Chen, X. (2022). A novel comprehensive agricultural drought index reflecting time lag of soil moisture to meteorology: A case study in the Yangtze River basin, China. *Catena*, 209(P1), 105804. <https://doi.org/10.1016/j.catena.2021.105804>
 74. Torres-Pineda, C.E., Pabón-Caicedo, J.D. (2017). Intraseasonal variability of precipitation in Colombia and its relationship with the Madden-Julian oscillation (in Spanish). *Revista de La Academia Colombiana de Ciencias Exactas, Físicas y Naturales*, 41(158), 79. <https://doi.org/10.18257/raccefyn.380>
 75. UPRA. (2018). Methodology for general identification of the agricultural frontier in Colombia (Metodología para la identificación general de la frontera agrícola en Colombia).
 76. Urrea, V., Ochoa, A., Mesa, O. (2019). Seasonality of Rainfall in Colombia. *Water Resources Research*, 55(5), 4149–4162. <https://doi.org/10.1029/2018WR023316>
 77. Vallat, R. (2018). *Pingouin: statistics in Python*. *Journal of Open Source Software*, 3(31), 1026. <https://doi.org/10.21105/joss.01026>
 78. Waliser, D.E., Jiang, X. (2015). Tropical Meteorology and Climate: Intertropical Convergence Zone. In *Encyclopedia of Atmospheric Sciences: Second Edition* (Second Edition, 6). Elsevier. <https://doi.org/10.1016/B978-0-12-382225-3.00417-5>
 79. Yue, S., Wang, C.Y. (2002). Applicability of prewhitening to eliminate the influence of serial correlation on the Mann-Kendall test. *Water Resources Research*, 38(6), 4-1-4-7. <https://doi.org/10.1029/2001wr000861>
 80. Zhang, H., Han, M., Comas, L.H., Dejonge, K.C., Gleason, S.M., Trout, T.J., Ma, L. (2019). Response of maize yield components to growth stage-based deficit irrigation. *Agronomy Journal*, 111(6), 3244–3252. <https://doi.org/10.2134/agronj2019.03.0214>
 81. Zhu, R., Hu, T., Wu, F., Liu, Y., Zhou, S., Wang, Y. (2023). Photosynthetic and hydraulic changes caused by water deficit and flooding stress increase rice's intrinsic water-use efficiency. *Agricultural Water Management*, 289, 108527. <https://doi.org/10.1016/j.agwat.2023.108527>
 82. Zi, L., Gargallo-Garriga, A., Oravec, M., AbdElgawad, H., Nijs, I., De Boeck, H.J., Reynaert, S., Donnelly, C., Li, L., Beemster, G.T.S., Urban, O., Asard, H. (2023). Ecometabolomic analysis of the effect of more persistent precipitation regimes reveals common and tolerance related metabolic adjustments in four grassland species. *Environmental and Experimental Botany*, 215, 105489. <https://doi.org/10.1016/j.envexpbot.2023.105489>